

Effects of Electron-Electron Scattering on Electron-Beam Propagation in a Two-Dimensional Electron-Gas

H. Predel, H. Buhmann, and L.W. Molenkamp

Physikalisches Institut der Universität Würzburg, D-97074 Würzburg, Germany

R.N. Gurzhi, A.N. Kalinenko, A.I. Kopeliovich, and A.V. Yanovsky

*B. Verkin Institute for Low Temperatures Physics & Engineering,
Nat.Acad of Sciences of Ukraine, Lenin Ave. 47, 31064, Kharkov, Ukraine*

We have studied experimentally and theoretically the influence of electron-electron collisions on the propagation of electron beams in a two-dimensional electron gas for excess injection energies ranging from zero up to the Fermi energy. We find that the detector signal consists of *quasiballistic* electrons, which either have not undergone any electron-electron collisions or have only been scattered at small angles. Theoretically, the small-angle scattering exhibits distinct features that can be traced back to the reduced dimensionality of the electron system. A number of nonlinear effects, also related to the two-dimensional character of the system, are discussed. In the simplest situation, the heating of the electron gas by the high-energy part of the beam leads to a weakening of the signal of quasiballistic electrons and to the appearance of thermovoltage. This results in a nonmonotonic dependence of the detector signal on the intensity of the injected beam, as observed experimentally.

72.10.-d;72.20.Dp

I. INTRODUCTION

The propagation of electron beams in the two-dimensional electron-gas (2DEG) of GaAs-(Al,Ga)As heterostructures was studied in a number of publications [1–5], and has proven to be a very sensitive tool for studying electron scattering-phenomena. In the first two Refs. [1,2], the emphasis was on the effects of *electron-phonon* scattering, where the beam was injected across tunnel barriers. These effects occur at relatively large excess energies of the electron beam, typically of the order of the optical phonon energy, some 30 meV. In later works [3,4], the effects of *electron-electron* scattering phenomena (occurring at much lower energies, typically below 10 meV) were analyzed, using opposite quantum point-contacts as injector and detector for the electron beam.

In our paper, Ref. [3], we paid much attention to thermal beams in which the characteristic energy of beam electrons ε , counted from Fermi level, is of the order of the sample temperature T_0 . It was shown that electron-electron collisions played a main role in damping such beams. The overall behaviour of the signal attenuation could be reasonably understood using the formula of Giuliani and Quinn [6] for the electron-electron scattering rate in a 2DEG, implying that the result of a single electron-electron collision is sufficient for an un-equilibrium electron to escape from detection (relaxation time approximation). This conclusion was subsequently confirmed by other groups [4,5].

In this work, we return to our studies of electron-electron scattering in a 2DEG system, equipped with a much more detailed framework of understanding of the dynamical scattering phenomena [7–11], which has first been used to explain the hydrodynamic electron flow-

phenomena we observed a few years ago [12]. These newly developed theories enable a much more refined analysis of the experimental data. Specifically targeting the theoretical predictions of Refs. [7–11] we have performed a new series of electron-beam experiments for different samples at various temperatures and for a wide range of injection energies. In our experiments we can identify specific two-dimensional effects, as well as novel nonlinearities due to 2DEG-heating. Our results cast doubts on the interpretations in Refs. [4] and [5].

In the course of this paper, we will first present the experimental results and their qualitative explanation (Sec. II). Next we develop a theoretical approach for the electron-beam propagation in small systems, i.e. where the probability of secondary collision is negligible (Sec. III), and for the opposite case, the multi-collision limit (the propagation of a beam over long distances becomes possible due to specific two-dimensional effects) (Sec. IV). In Sec. V we consider non-linear phenomena which can play an essential role for the interpretation of an electron-beam signal and we analyse the experimental data in the framework of the here developed theory in Sec. VI. Throughout this paper we will use 'energy-units' for temperature and potential differences, i.e. the Boltzmann constant k_B and the electron charge e are equal to one.

II. EXPERIMENT

The experiments were performed on gate-defined nanostructures in conventional modulation doped GaAs-(Al,Ga)As heterojunctions. Typical values for the carrier density and mobility are $n_e = 2.45 \times 10^{11} \text{ cm}^{-2}$ and

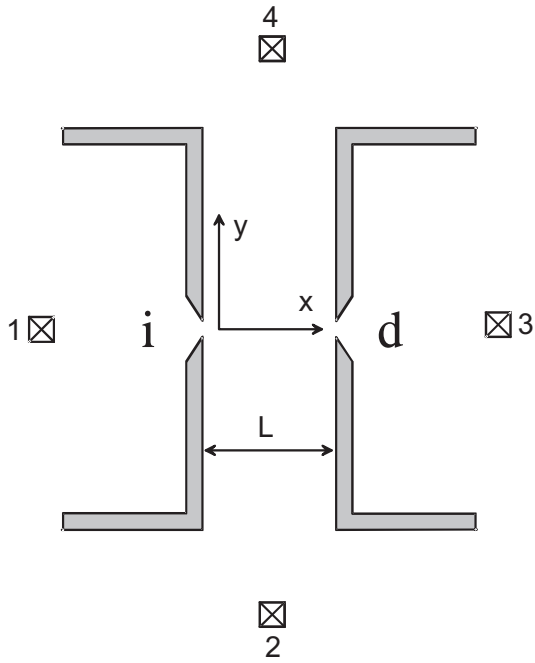


FIG. 1. Schematic topview of the device layout. Hatched areas are Schottky gates, defining the device geometry, crossed squares denote Ohmic contacts, i and d symbolize the injector and detector quantum point-contact, respectively.

$\mu \approx 1 \times 10^6 \text{ cm}^2(\text{Vs})^{-1}$, corresponding to an impurity mean-free-path of $l_{\text{imp}} \approx 20 \mu\text{m}$. A schematic topview of the sample gate-structure is given in Fig. 1. Schottky gates (grey areas) form two opposite quantum point-contacts, i and d , at lithographical distances of $L = 0.6, 2, 3.4,$ and $4 \mu\text{m}$ for different samples.

In the experiments, the electron beam was injected through the injector quantum point-contact i by applying a dc voltage $V_i = V_{12}$ and detected as the non-local voltage $V_d = V_{34}$ across the detector point-contact d . The numbers 1, 2, 3, and 4 denote the Ohmic contacts to the 2DEG of the sample (Fig. 1, crossed squares). We stress that the use of all-dc techniques is very important for a proper interpretation of the observed signals. Differential resistance measurements with lock-in techniques will not elucidate the role of the thermovoltage background to the signal in full. Both injector and detector point-contacts were adjusted at the $n = 1$ plateau i.e., both contain one transverse mode, and thus remain in the metallic regime, $G_{\text{QPC}} = n2e^2/h$. (In other words, they do not act as tunnel barriers, as was the case in Refs. [1,2].) Thus, electrons of all possible energies, $0 < \varepsilon < V_i$, are present in the injected beam.

In the presence of a magnetic field perpendicular to the 2DEG plane, the electron beam is deflected and the detector signal, $V_d(B)$ yields the beam profile (see Fig. 2). For the present a point-contact adjustment at $n = 1$ and a injector-detector distance $L = 3.4 \mu\text{m}$ we obtain the characteristic opening angle of injector and detector which amounts to $\phi \sim 18^\circ$ (cf. [15]).

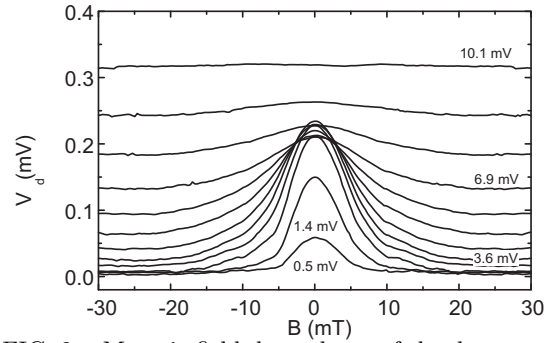


FIG. 2. Magnetic-field dependence of the detector signal V_d for different injection voltages: 0.5, 1.4, 2.2, 2.9, 3.6, 4.4, 5.5, 6.0, 6.9, 7.8, 8.8, and 10.1 mV (bottom to top). Note that no offset is added to the experimental data.

From Fig. 2, showing the $V_d(B)$ -dependence for different injection energies ($0.5 \leq V_i \leq 10 \text{ mV}$) at 1.6 K, one can see that the detector signal first increases with increasing injector voltage. Then for $V_i > 3 \text{ mV}$ a strong increase of a isotropic background signal is observed while at the same time the beam profile broadens. For injection energies larger 10 meV a beam signal can hardly be resolved, while the background increases continuously.

To investigate the effects of electron-electron scattering events on the beam propagation we are interested in the dependence of detector-signal on the injection energy at $B = 0$. Fig. 3 a) presents the experimental results for the sample $L = 3.4 \mu\text{m}$ at three different sample temperatures, $T_0 = 1.6, 8$ and 11 K . Additional measurements (not shown here) were made at different sample (lattice) temperatures, $T_0 = 2.2, 3.4, 5, 15,$ and 17 K and for different injector-detector distances. It can be seen from Fig. 3 a) that for low injection energies the detector signal increases linearly with V_i . For $V_i > 3 \text{ meV}$ only for the lowest temperature (curve 1) a saturation and even a small decrease is observed. For high injection energies the $V_d(V_i)$ dependence increases for all temperatures.

As we have seen from Fig. 2, for $V_i > 3 \text{ meV}$ an increasing isotropic background signal is detected, which is not directly related to the ballistic electron-beam propagation. In order to extract the ballistic part of the detector signal we measured the isotropic background signal separately by repeating the experiment for high magnetic fields ($B = 50 \text{ mT}$) to ensure that the electron beam is totally deflected and ballistic beam electrons do not contribute to the detector signal [Fig. 3 b)]. Subtracting this background signal from the data measured for $B = 0 \text{ T}$ we obtain the pure electron-beam contribution to the detector signal [Fig. 3 c)]. Now the result is similar for all temperatures: We observe first a linear increase of V_d with increasing V_i and then a saturation followed by a decrease for high injection energies, while with increasing sample temperature the maximum electron-beam signal decreases [Fig. 3 c)].

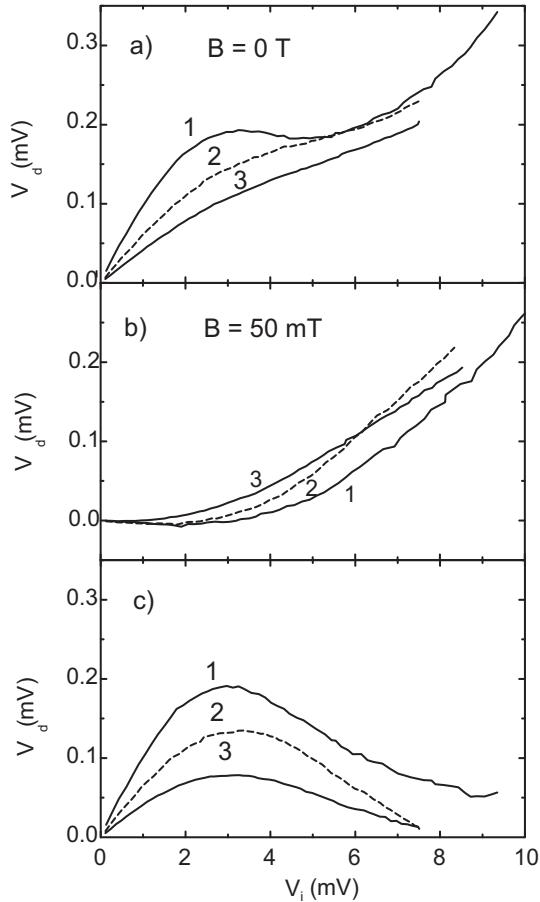


FIG. 3. Experimental dependence of the detector signal V_d on the injector voltage V_i for $L = 3.4 \mu\text{m}$ at three different sample temperatures $T_0 = 1.6 \text{ K}$ (trace 1), 8.0 K (trace 2), and 11 K (trace 3). (a) detector signal at zero magnetic field - electron beam is directed straight from injector to detector, (b) $B = 50 \text{ mT}$ - the electron beam is deflected and does not reach the detector directly [isotropic background signal (thermovoltage)]. (c) Contribution of narrow-directed (quasiballistic) movement of electrons to the detector signal resulting from subtracting the appropriate data sets of Fig. 2 b) from Fig. 2 a) [$T_0 = 1.6 \text{ K}$ (trace 1), 8.0 K (trace 2), and 11 K (trace 3)].

These experimental results can be understood from the following qualitative considerations. Let us assume, for simplicity, that the lattice temperature (the primary temperature of the system) is equal to zero. Then, for a nonequilibrium electron with excess energy ε above the Fermi energy ε_F , the mean-free-path for collisions with equilibrium electrons decreases with increasing ε , roughly speaking as $l_{ee}(\varepsilon) \sim \varepsilon^{-2} \ln \varepsilon^{-1}$, $\varepsilon \ll \varepsilon_F$ [13]. Therefore, at sufficiently small V_i all injected electrons will reach the detector, whose readout then is proportional to the number of injected electrons, $V_d \propto V_i$, schematically shown in Fig. 4. (Electrons of all energies $0 \leq \varepsilon \leq V_i$ are present in the beam, with equal weight). This linear increase of V_d with V_i saturates for energies $\varepsilon \geq \varepsilon_0$ when the electron-

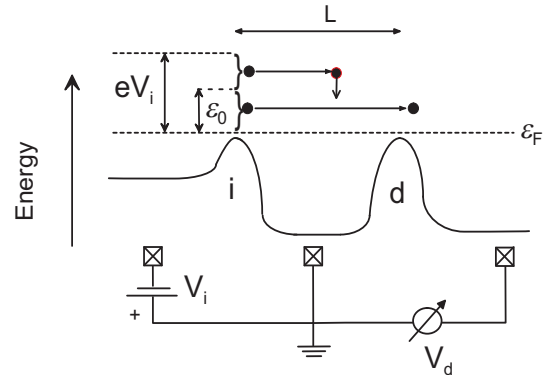


FIG. 4. Schematic view of the characteristic energies of the electron-beam experiments. Potential barriers are shown at the center of the quantum point-contacts. Typical energies are indicated: ε_F (Fermi energy), eV_i (injection energy), and ε_0 [maximum energy for electrons reaching the detector ballistically ($l(\varepsilon_0) = L$)]. Note, the effective charging of the area behind the detector (eV_d) is at least 30 times smaller than the injection energy and therefore negligible on the scale of this diagram.

electron scattering mean free path length (l_{ee}) becomes comparable to L , the distance between injector and detector: $V_i = \varepsilon_0$ for $l_{ee}(\varepsilon_0) = L$. Electrons with larger energies, $\varepsilon_0 < \varepsilon < V_i$, will scatter and do not reach the detector. Thus, the signal V_d is determined by a fraction of electrons which is completely saturated at $V_i \sim \varepsilon_0$ and should not change on a further increase of V_i . However, as is evident from Fig. 3 a), the signal, upon reaching a maximum, starts to decrease slightly. The only possible mechanism leading to such behaviour is heating of the 2DEG in between injector and detector point-contact by the electron beam. The heated 2DEG then leads to damping of the electron beam due to enhanced electron-electron scattering. At still higher V_i , V_d shows again an increase [Fig. 3 a)]. This is due to the additional build-up of a thermovoltage across the detector point-contact [Fig. 2 and 3 b)], which is driven by the temperature difference between the heated 2DEG in between injector and detector and the still cold 2DEG behind the detector [16].

As we will see below, the qualitative picture given above is fully confirmed by the theory described in this work. We will demonstrate that under our experimental conditions it is possible to separate the electrons of the beam into two groups, i.e. "quasiballistic" ($\varepsilon < \varepsilon_0$) and "heating electrons" ($\varepsilon > \varepsilon_0$), which greatly simplifies the interpretation of the experimental results.

III. ONE-COLLISION APPROXIMATION

The detected signal V_d is determined by the distribution function of nonequilibrium electrons f in the vicinity

of detector point-contact. For now, we neglect nonlinearities due to heating of the 2DEG in between injector and detector, which is a valid approximation for sufficiently low excess energies of the injected electrons. The linearized Boltzmann equation, describing the behaviour of the distribution function f , then has the form

$$v_x \frac{\partial f}{\partial x} + v_y \frac{\partial f}{\partial y} = \hat{J}f, \quad f(x=0, y, \mathbf{p}) = f_0(y, \mathbf{p}) \quad (1)$$

Here, $f_0(y, \mathbf{p})$ is the beam profile at the exit from the injector, and the axis x is directed from injector to detector (cf. Fig. 1). $\hat{J}f$ is a linearized integral describing the electron-electron collisions. It is convenient to write it as

$$\hat{J}f = -\nu f + \int d\mathbf{p}' \nu_{\mathbf{p}\mathbf{p}'} f_{\mathbf{p}'}, \quad \nu = \int d\mathbf{p}' \nu_{\mathbf{p}\mathbf{p}'}. \quad (2)$$

Here, the collision-integral kernel $\nu_{\mathbf{p}\mathbf{p}'}$ determines the probability of the appearance of a nonequilibrium electron ($\nu_{\mathbf{p}\mathbf{p}'} > 0$) or hole ($\nu_{\mathbf{p}\mathbf{p}'} < 0$) in state \mathbf{p}' after the nonequilibrium electron has disappeared from state \mathbf{p} (i.e., has been scattered into another state). The kernel has a complex structure and in the general case can not be presented in elementary functions. We have

$$\nu_{\mathbf{p}\mathbf{p}'} = \frac{1}{n(\varepsilon)} \int d\mathbf{p}_1 d\mathbf{p}_2 (2 \Psi_{\mathbf{p}'\mathbf{p}_1\mathbf{p}\mathbf{p}_2} - \Psi_{\mathbf{p}'\mathbf{p}\mathbf{p}_1\mathbf{p}_2}) \quad , \quad (3)$$

where

$$\Psi_{\mathbf{p}'\mathbf{p}\mathbf{p}_1\mathbf{p}_2} = W_{\mathbf{p}'\mathbf{p}\mathbf{p}_1\mathbf{p}_2} (1 - n(\varepsilon')) n(\varepsilon_1) n(\varepsilon_2) \times \delta(\mathbf{p}' + \mathbf{p} - \mathbf{p}_1 - \mathbf{p}_2) \delta(\varepsilon' + \varepsilon - \varepsilon_1 - \varepsilon_2). \quad (4)$$

Here $W_{\mathbf{p}'\mathbf{p}\mathbf{p}_1\mathbf{p}_2}$ is proportional to the square of the matrix element of the electron-electron interaction, and $n(\varepsilon)$ is the equilibrium Fermi distribution function.

We now introduce the angular scattering distribution function:

$$g(\varphi) = \nu^{-1} m \int d\varepsilon' \nu_{\mathbf{p}\mathbf{p}'}, \quad (5)$$

where φ is the scattering angle. For simplicity, we assume parabolic bands ($\varepsilon = p^2/2m$), which is a good approximation for the conduction band in GaAs-(Al,Ga)As heterostructures. At sufficiently small ε and T , the form of $g(\varphi)$ is determined mainly by the phase-space restraints imposed by the two-dimensional character of the 2DEG [7–10]. Roughly speaking, $g(\varphi)$ consists of a narrow bunch of electrons flying forward in an angle range of the order of $\pm(\varepsilon + T)^{1/2} \varepsilon_F^{-1/2}$ and a bunch of holes, of approximately the same width, flying backward (see Ref. [11]). Therefore, the electron-electron scattering is effectively a small-angular process [7–9].

For the general case, Eq. (1) can not be solved. However, under conditions where the probability of collisions is small, i.e. $l_{ee} = v(\varepsilon)\nu^{-1}(\varepsilon) \gg L$, or $\varepsilon \ll \varepsilon_0$, we can use perturbation theory for the collision integral. In the first order or one-collision approximation we then have

$$\begin{aligned} f(x, y, \mathbf{p}) &= \left(1 - \frac{x\nu}{v_x}\right) f_0\left(y - \frac{v_y}{v_x}x, \mathbf{p}\right) + \\ &+ \frac{1}{v_x} \int_0^x dx' \int d\mathbf{p}' \nu_{\mathbf{p}\mathbf{p}'} f_0\left[y - \frac{v_y}{v_x}x + \left(\frac{v_y}{v_x} - \frac{v'_y}{v'_x}\right)x', \mathbf{p}'\right] \equiv \\ &\equiv \left(1 - \frac{x\nu}{v_x}\right) f_0 + \hat{Q}f_0. \end{aligned} \quad (6)$$

The first term on the r.h.s of Eq. (6) describes the number of nonscattered particles reaching into the vicinity of a point (x, y) . The second (integral) term $\hat{Q}f_0$ describes particles that reach the same spatial region, after having been scattered once.

Note that for high-energy beams ($\varepsilon \gg T$), the probability of undergoing a second collision is approximately one order of magnitude lower than that of the first collision [10]. This is connected with the fact that after collision with equilibrium (Fermi sea) electrons, the excess energy of a nonequilibrium electron (ε) must be redistributed between three partners i.e., $\bar{\varepsilon} \approx \varepsilon/3$, $l_{ee}(\bar{\varepsilon}) \approx 3^2 l_{ee}(\varepsilon)$, $T \ll \varepsilon \ll \varepsilon_F$, where $\bar{\varepsilon}$ is the characteristic energy of the scattered electrons. Therefore, the one-collision approximation is valid for a relatively wide range of energies as long as $l_{ee}(\bar{\varepsilon}) \geq L$. On observing this and the fact that $\hat{Q}\nu f_0 \sim \nu(\varepsilon)\hat{Q}f_0 \gg \nu\hat{Q}f_0 \sim \nu(\bar{\varepsilon})\hat{Q}f_0$, it is straightforward to build a new "modified" one-collision approximation. After partial summation of the terms of the iteration series on the parameter $x/l_{ee}(\varepsilon)$ of Eq. (1) one obtains the following expression in zero-th order approximation for the parameter $x/l_{ee}(\bar{\varepsilon})$:

$$\begin{aligned} f &\approx e^{-\frac{x\nu}{v_x}} f_0\left(y - \frac{v_y}{v_x}x, \mathbf{p}\right) + \\ &+ \frac{1}{v_x} \int_0^x dx' \int d\mathbf{p}' \nu_{\mathbf{p}\mathbf{p}'} e^{-\frac{\nu(\varepsilon')x'}{v'_x}} \\ &\times f_0\left[y - \frac{v_y}{v_x}x + \left(\frac{v_y}{v_x} - \frac{v'_y}{v'_x}\right)x', \mathbf{p}'\right]. \end{aligned} \quad (7)$$

This formula is valid when $\varepsilon < 3\varepsilon_0$. The first term on the r.h.s. corresponds to the usual relaxation-time approximation, $\hat{J}f = -\nu f$. Note that the modified one-collision approximation Eq. (7) is based on an exact consideration of the first collision and not on perturbation theory. It does not take into account any further collisions.

The experimentally measured voltage drop, V_d , is determined by the current passing the detector point-contact and can be calculated from

$$V_d = e \int d\varepsilon \int d\varphi \rho(\varphi) v_x f(x=L, y=0, \mathbf{p}). \quad (8)$$

Here $\rho(\varphi)$ is the function characterizing the angular acceptance of the detector point-contact, which is positioned at $(L, 0)$. For simplicity, we use in our numerical calculations Heaviside step-functions to represent the angular characteristics of injector and detector point-contacts:

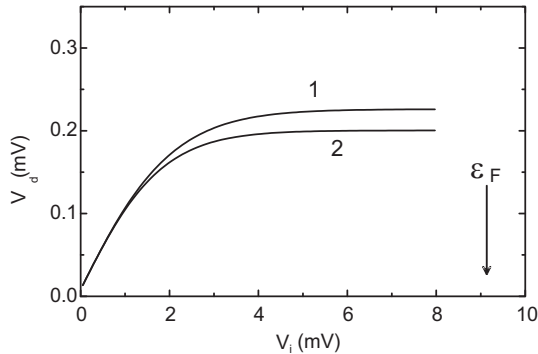


FIG. 5. Calculated $V_d(V_i)$ dependences without taking into account electron heating of the 2DEG in between injector and collector. Curve 1: Modified one-collisional approximation Eqs.(7),(8); curve 2: relaxation-time approximation; with $\phi = 18^\circ$, $L = 3.4 \mu\text{m}$, $\varepsilon_0 = 0.2 \text{ meV}$, and $\varepsilon_F = 9 \text{ meV}$.

$$\rho(\varphi) \propto \theta(\phi/2 - |\varphi|) \quad (9)$$

$$f_0(y, \mathbf{p}) \propto \theta(\phi/2 - |\varphi|) \theta(V_i - \varepsilon).$$

In this model, the behaviour of $V_d(V_i)$ is determined by two parameters, i.e. the angular injection (and acceptance) range of the point-contact ϕ and the distance between injector and detector L . For more realistic models of the angular response of quantum point-contacts we refer to Ref. [15].

The dependence $V_d(V_i)$ is calculated using Eqs. (7-9), including the expressions for the kernel $\nu_{\mathbf{p}\mathbf{p}'}$ obtained in Ref. [11], setting $\phi = 18^\circ$, and $L = 3.4 \mu\text{m}$, i.e. close to the experimental conditions. The result is shown in Fig. 5 for the full expression of the modified one-collision approximation (MOCA) (curve 1) and the relaxation-time approximation (RTA) (curve 2). We clearly observe that the curves saturate with increasing V_i . Saturation occurs at a higher injection voltage, V_i , and a higher signal level, V_d , for the MOCA as compared with the RTA. The difference between these curves (about 15 %) characterizes the role of two-dimensional effects for the given parameters. This difference is due to the integral term in Eq. (7), which can be omitted when 2D effects are negligible.

In the next section we show that the role of the two-dimensionality is much larger when $\phi > (\varepsilon_0/\varepsilon_F)^{1/2}$. In this limit, a saturation of the curve at $V_i < 3 \varepsilon_0$ does not take place at all.

IV. MULTI-COLLISION REGIMES

In the limit where the electrons undergo a number of collisions on their way from injector to detector, it is impossible to obtain a completely analytical solution of the spatially-inhomogeneous problem of beam propagation. Instead, we will discuss below a simple qualitative theory that adequately describes this multi-collision regime.

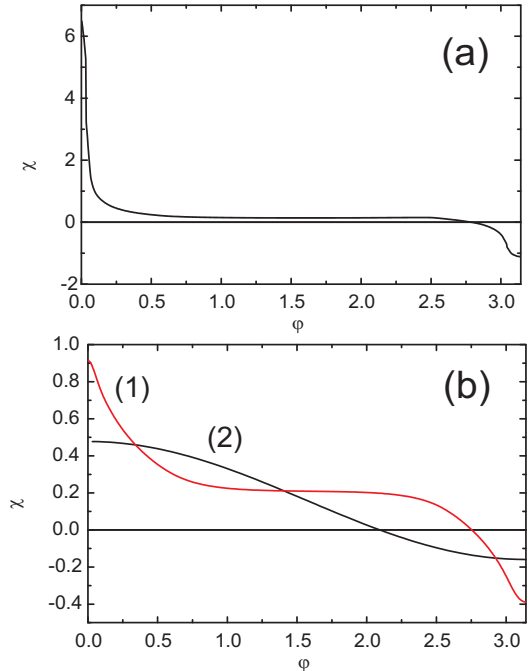


FIG. 6. The temporal evolution of a thermalized spatially-uniform distribution $\chi(t, \varphi)$ [$T/\varepsilon_F = 0.1$ and $\chi|_{t=0} \propto \delta(\varphi)$]. (a) $t = \tau_{ee}$; (b) $t = 10 \tau_{ee}$ (curve 1). Curve 2 for comparison the 3D case after a few electron-electron collisions (drift-like distribution).

To obtain realistic numerical values of the angular relaxation rate we first consider the momentum relaxation in time for a spatially homogeneous distribution. For simplicity, we take the thermalized distribution $f = (-\partial n/\partial \varepsilon)\chi(\varphi, t)$, i.e. equilibrium is established in energy but not in momentum. In this case the kernel of the collision integral contains only differences in the angular variables, and the solution of the Boltzmann equation reduces to the calculation of a one-dimensional Fourier transform. Here, we use the numerical results of the angular distribution function $g(\varphi)$ that were obtained in Ref. [11]. (In the case of non-thermalized distributions the angular and energy variables are not separable and therefore the solution of the Boltzmann equation becomes a much more difficult problem.) Fig. 6 shows the results of a calculation for thermalized conditions at $T_0 = 0.1 \varepsilon_F$ and for different times t after beam injection. From this figure follows that the beam remains narrow up to times of the order of $10 \tau_{ee}$, whereas in the three-dimensional case a smooth drift-like distribution is already established after a delay of the order of one collision-time. From now on, we will use the convention $0.1 \varepsilon_F \equiv \varepsilon^*$ to denote the characteristic energy of a beam, below which the specific features of two-dimensional relaxation essentially manifest themselves.

Depending on the relative magnitude of ε_0 and the temperature T of the 2DEG, different multi-collision regimes are possible:

1. Let us start with the case of low temperatures, $T \ll \varepsilon_0$. We assume that L is so large that $\varepsilon_0 < \varepsilon^*$. In this case, the particles that undergo multiple collisions but still contribute to the electron beam signal, are those whose mean-free-path is considerably less than L and whose scattering is small-angular:

$$\varepsilon_0 < \varepsilon < \varepsilon^*. \quad (10)$$

Note that after a few collisions the energy of such particles drops very rapidly to values close to ε_0 , upon which the particles will reach the detector without further collision. In contrast, the opening angle broadening α of the electron beam is determined by the first collision $\alpha \sim \sqrt{\varepsilon/\varepsilon_F} \ll 1$. It is then straightforward to evaluate the contribution to the detector signal of the group of electrons with energies in the range $(\varepsilon_0, \varepsilon)$:

$$V_d \sim (\varepsilon - \varepsilon_0) \frac{\lambda_F}{r_\perp} \frac{\phi}{\alpha} \sim \varepsilon_F \frac{\varepsilon - \varepsilon_0}{\varepsilon} \frac{\lambda_F}{L} \phi. \quad (11)$$

The transverse beam broadening is $r_\perp \simeq L\alpha$. The detector width is chosen to be of the order of the electron Fermi wave-length λ_F (corresponding to the occupation of one mode in the quantum point-contact). We have assumed an angle of acceptance $\phi \ll \alpha$ for the detector point-contact [15]; in the other case, if $\phi \geq \alpha$, the multiplier ϕ/α can be omitted for the above expression.

The order of magnitude of the contribution of ballistic electrons to the detector signal can be estimated as $V_d \sim \varepsilon_0 \lambda_F (L\phi)^{-1}$, where we assume identical characteristics for injector and detector quantum point-contacts. Therefore, the condition for a predominance of the group of non-ballistic electrons to the detector signal takes the form

$$\phi > \sqrt{\frac{\varepsilon_0}{\varepsilon_F}}. \quad (12)$$

This inequality is satisfied more easily for samples with larger L (i.e. smaller ε_0) or larger acceptance angles ϕ . Under our experimental conditions the l.h.s. and r.h.s. in Eq. (12) coincide by an order of magnitude, and it turns out that the 2D effects lead to corrections of the order of unity. In case $\phi \gg \sqrt{\varepsilon_0/\varepsilon_F}$ it should be possible to observe the long-distance beam propagation as predicted in Ref. [8]. In other words, one can detect an electron beam over a distance exceeding substantially the electron-electron mean-free-path l_{ee} as a result of one-dimensional electron-hole diffusion.

2. For $\varepsilon_0 \ll T$, ballistic electrons are practically absent. Roughly speaking, the number of quasi-particles reaching the detector without any collisions is exponentially small and proportional to $\exp[-L/l_{ee}(T)] = \exp(-T^2\varepsilon_0^{-2})$. High-energy electrons with energies $\varepsilon_F > \varepsilon > T$ lose their excess energy very quickly, after a few collisions, and cool down to energies of the order of the lattice temperature T . Simultaneously, the beam acquires an angular broadening of the order of

$\sqrt{\varepsilon/\varepsilon_F} < 1$. After this initial relaxation, provided $T < \varepsilon^*$, we still have a narrow distribution of electrons (and holes with opposite momenta) whose movement is a one-dimensional diffusion in coordinate space – an effect which is genuinely caused by the two-dimensionality of the electron system. The angular broadening in time of this specific group can be expressed as $\alpha \sim \sqrt{T/\varepsilon_F} [t/\tau_{ee}(T)]^{1/4}$ (cf. [7,10]). The contribution of this narrowly-directed group of electrons to the detected signal can be evaluated using Eq. (11). Taking into account, that, assuming one-dimensional diffusion, the time an electron needs to reach from injector to detector is of the order of $v_F^{-1} L^2 l_{ee}^{-1}(T)$ we obtain

$$\alpha \sim \sqrt{\varepsilon/\varepsilon_F} + \sqrt{T/\varepsilon_F} [L/l_{ee}(T)]^{1/2}, \quad (13)$$

$$r_\perp \sim L \left\{ \sqrt{\varepsilon/\varepsilon_F} + \sqrt{T/\varepsilon_F} [L/l_{ee}(T)]^{3/2} \right\}.$$

As one can see from these expressions, the result of Eq. (11) obtained above is retrieved for $\varepsilon > T^3\varepsilon_0^{-2} \equiv T^*$. At the same time, the contribution to the detector signal of electrons with energies $T_0 < \varepsilon < T^*$ is given by

$$V_d \sim \varepsilon \frac{\lambda_F l_{ee}^2(T)}{L^3} \frac{\varepsilon_F \phi}{T}. \quad (14)$$

According to Eqs. (11) and (14), the signal decreases with increasing L according to a power-law, but not exponentially. This again is essentially a two-dimensional effect (cf. [8,9]) and should be well-pronounced in high-mobility samples with sufficiently large L .

Thus, it is possible to create conditions in a two-dimensional electron-gas under which the electron-beam signal is determined rather by a higher-energy quasiballistic group of electrons which experience small-angle scattering than by purely ballistic electrons $\varepsilon \leq \varepsilon_0$.

V. NON-LINEAR EFFECTS AND HEATING

Due to the heating of the electron gas between injector and detector point-contacts for 'high' excess energies the detector signal consists not only of quasiballistic beam electrons but also of an isotropic signal resulting in a thermovoltage across the detector. This causes the growth of V_d for injection energies $V_i > 5$ mV in our experiments [Fig. 3 a) and b)]. The contribution of the thermopower to the detector signal is given by

$$\Delta V_d = S(T)\Delta T, \quad \Delta T = T - T_0. \quad (15)$$

Here, T is the electron gas temperature between injector and detector and T_0 is the gas temperature beyond the detector (which is close to the lattice temperature), $S(T)$ is the Seebeck coefficient (thermopower) of the detector (heating of the 2DEG between injector and detector by the injected electron beam was already discussed by us in Ref. [3]). As discussed above (Sec. II), on increasing V_i , the increase of T leads to an increase of the

thermoelectric voltage on the one hand, and to the decrease of the mean-free-path of quasiballistic electrons on the other hand, and therefore to the appearance of minimum in the dependence $V_d(V_i)$.

For $\varepsilon_0 > \varepsilon^*$ (the limit where specific 2D effects can be neglected), only ballistic electrons contribute to the beam signal. We then have as a rough estimate for the temperature dependence of the signal:

$$V_d(T) \sim \kappa e^{-\frac{L}{l_{ee}(T)}} + S(T)\Delta T, \quad \kappa^{-1} \sim L\lambda_F^{-1}\phi(V_i^{-1} + \varepsilon_0^{-1}). \quad (16)$$

An analysis of this expression shows that a minimum in $V_d(T)$ is always present when $V_i > \varepsilon_0$. This statement holds as well in the multi-collision regime $\varepsilon_0 < T < \varepsilon^*$ [see Eq. (14)]. It is evident that with increasing V_i the temperature of the 2DEG between injector and detector point-contact increases. However, this does not necessarily imply that the $V_d(V_i)$ dependence replicates $V_d(T)$ of Eq. (16) qualitatively, because V_i enters explicitly in Eq. (16) and not only through $T(V_i)$. One can only state definitely that the beam signal should decrease sooner or later on increasing V_i .

Generally speaking, the theoretical determination of the dependence $T(V_i)$ requires solving a complex nonlinear problem on the beam's self-action. However, the essential dependence of the mean-free-path on excess energy allows considerable simplifications for sufficiently high V_i , i.e., the separation of the injected particles in (i) "heating" (high-energy electrons which do not reach the detector) and (ii) quasiballistic electrons (which contribute mainly to the beam signal, but not to heating). Such a separation is undoubtedly possible at $V_i > \varepsilon_0 > \varepsilon^*$. (If $V_i \leq \varepsilon_0$ we can neglect heating.)

Thus, under certain conditions one can use the following quasi-linear approach: First, we find the electron gas heating $\Delta T(V_i)$ due to the high-energy part of the beam, and then, using the electron temperature T thus obtained, we determine the signal of the quasiballistic part. In particular, in the relaxation-time approximation we have:

$$f = e^{-\frac{L}{v_x \tau_{ee}(\varepsilon, T)}} f_0 \left(y - L \frac{v_y}{v_x}, \mathbf{p} \right), \quad (17)$$

where $T = T_0 + \Delta T(V_i)$. In fact, this means that the separation reduces the nonlinear problem to two linear equations.

Finally, we want to consider the case when $\varepsilon_0 < V_i < \varepsilon^*$ where, due to the specific two-dimensional effects, the injected particles slowly relax their directionality, but rapidly lose their excess energy [7]. In this limit, it is not possible to separate heating particles from quasiballistic ones. The beam signal is proportional to $l_{ee}^2(T)T^{-1}$ [see Eq. (14)] and, hence, it is sensitive to heating. This essentially nonlinear situation could be realized experimentally for high quality samples with a large distance L between injector and detector.

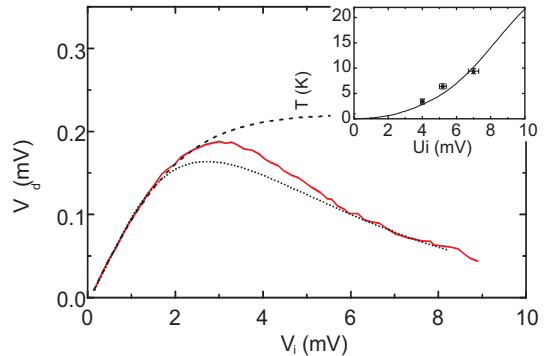


FIG. 7. The comparison of theory and experiment for $T_0 = 1.6$ K: modified one-collision approximation (dashed line), the experiment (solid line), and the relaxation-time approximation with taking into account the heating (dotted line). The inset displays the dependence of the electron temperature on injector voltage, $\Delta T(V_i)$, obtained from heating temperature measurements (solid line) and from the experimentally determined temperature dependence of the detector signal (Fig. 3) (squares).

VI. DISCUSSION OF THE EXPERIMENT

In this section we want to compare the experimental results, Sec. II, with our theoretical results. A series of measurements for different sample temperatures, $T_0 = 1.6, 2.2, 3.4, 5.0, 8.0, 11, 15, \text{ and } 17$ K were available for analysis (partly shown in Fig. 3). For temperatures $T_0 < 8$ K, the modified one-collision approximation [Eqs. (7), (8) and (9)] allows a proper description of the experiment for $V_i < 3$ mV, see Fig. 4 (note that $l_{ee} \approx L = 3.4 \mu\text{m}$ for $V_i = \varepsilon_0 \simeq 2$ mV). For higher values of V_i , where heating is essential, one can use the relaxation-time approximation [Eq. (17)], taking into account the $T(V_i)$ dependence].

To compare theory with experiment we extract the heating $\Delta T(V_i)$ in two different ways: First, by measuring the heating caused by the electron beam as a function of injection energy, using the thermoelectric voltage across the detector quantum point-contact as a thermometer [17] and second, by analysing the set of experimental data for the anisotropic part of the signal (Fig. 3), see below.

The result of an electron-temperature measurement determined via thermopower for a lattice temperature $T_0 = 1.6$ K is displayed in the inset of Fig. 7. Here, the detector point-contact conductance was adjusted to yield a maximum thermopower ($S \approx 20 \mu\text{V/K}$) [17], where the conductance of the injector point-contact was fixed at one mode so that its thermopower is negligible compared with the detector. The measurements were done at small magnetic fields ($B = 50$ mT) to prevent beam electrons from reaching the detector point-contact directly.

Alternatively, the decrease of the detector signal due to the quasiballistic part of the electron beam allows for an estimate of the 2DEG beam heating. We assume

that the part of these curves at values V_i larger than the injector voltage at the maximum in V_d (which we now denote as V_i^{\max}) describes the signal from the full narrowly-directed fraction of electrons as a function of 2DEG temperature, i.e. $V_d(T_0 + \Delta T(V_i))$. Thus, the curves in Fig. 3 are members of a one-parameter family which differ only by the value of the temperature T_0 . For the validity of this statement, it is important that heating can be neglected at the local maximum of $V_d(V_i)$ for each curve, $\Delta T(V_i^{\max}) \approx 0$. From Fig. 3 b) it is evident that at V_i^{\max} the thermovoltage is indeed negligible. Let us now consider any two curves T_{01} and T_{02} of this family and let $T_{01} < T_{02}$. Then curve T_{01} has always larger values V_d for a given V_i than curve T_{02} , and curve T_{01} decreases to a signal V_d , equal in size to the maximum of curve T_{02} at a given, larger, value of V_i . Now, it is evident that $T_{01} + \Delta T(V_i) = T_{02}$. In this manner, we are able to reconstruct the function $\Delta T(V_i)$. Let us emphasize, that it is convenient to choose the local maximum V_i^{\max} as a starting point for recovering $\Delta T(V_i)$, since, in the vicinity of this point there is no need (i) to correct for the increase of the signal due to the quasiballistic group of electrons with increasing V_i , that takes place at low V_i in the linear response regime, and (ii) to take heating effects into account. As an example, let us consider the curves 1 and 2 of Fig. 3, i.e., $T_{01} = 1.6$ K and $T_{02} = 8$ K. The maximum value of curve 2 is approximately 0.135 mV. The same value of V_d for curve 1 is reached in decreasing part of the curve at $V_i \sim 5.2$ mV. Thus, we obtain a heating temperature of $\Delta T \simeq T_{02} - T_{01} = 6.4$ K for $V_i \sim 5.2$ mV. The results obtained for the experiments at the lowest sample temperature $T_0 = 1.6$ K are shown in the inset of Fig. 7 (squares). It can be seen that the extracted heating temperatures agree well with 2DEG temperature measurements for applied magnetic fields. We therefore can use this $T(V_i)$ -dependence for further considerations. Note that the heating temperature depends not only on V_i but also on the initial sample temperature T_0 : $\Delta T = \Delta T(V_i, T_0)$. For higher T_0 , the 2DEG heating is less efficient, cf. Fig. 3.

Additionally, the electron temperature can be estimated roughly from the heat-balance between the energies transferred from the electron beam into the 2DEG and removed by phonons [14]. We then have

$$v_F < \varepsilon > \lambda_F \frac{V_i}{\varepsilon_F} n_e \sim \nu_{ep} s \hbar k_F \frac{T}{\varepsilon_F} n_e \Sigma. \quad (18)$$

Here, $< \varepsilon > \sim V_i/2$ is the average energy of the electron beam, $n_e V_i / \varepsilon_F$ is the number of injected electrons, ν_{ep} is the frequency of electron-phonon collisions, s is the sound velocity, k_F is the Fermi wave vector, and Σ is the area of the heated 2DEG region. Thus, we obtain for the electron temperature

$$T \sim \frac{\lambda_F l_{ep}}{\Sigma} \frac{\varepsilon_F}{s \hbar k_F} < \varepsilon >. \quad (19)$$

In order to evaluate this expression we assume for the experimental situation the following values: $s \sim 6 \times 10^5$

cm s⁻¹, $k_F = 1.18 \times 10^6$ cm⁻¹, $\varepsilon_F = 9$ mV, and Σ is taken to be of the order of the area between injector and detector, viz. $200 \mu\text{m}^2$. The mean-free-path for electron-phonon collisions l_{ep} is estimated at $100 \mu\text{m}$, yielding $T(V_i = 5.2 \text{ mV}) \simeq 7.3$ K [Eq. (19)]. In spite of this very crude model, we thus find a remarkable agreement with the electron temperature obtain from the experimental data ($\Delta T(V_i \simeq 5.2 \text{ mV}) = 6.4$ K).

As mentioned above, the experimental data can be approximated using the modified one-collision approximation [Eq. (7)] for injection energies $V_i < V_i^{\max}$ and the relaxation-time approximation [Eq. (17)] for V_i which is sufficiently large in comparison with V_i^{\max} . At high $T(V_i)$ the scattering is not small-angular and leads to a more or less isotropic background, i.e. 2D effects are absent. According to this, we plotted in Fig. 7 the modified one-collision approximation (dashed line), experiment (solid line) for $T_0 = 1.6$ K and the relaxation-time approximation (RTA) (dotted line), which takes into account electron-heating effects. For the RTA we have use the asymptotic expression

$$\tau_{ee}^{-1}(\varepsilon, T) = \frac{\varepsilon^2 + 2\pi^2 T^2}{4\pi \hbar \varepsilon_F} \ln \frac{\varepsilon_F}{T + \varepsilon}, \quad (20)$$

which is valid for arbitrary ratio of small values of T/ε_F and $\varepsilon/\varepsilon_F$ [9]. The coefficients for the theoretical calculations were chosen in such a way that coincidence is achieved for small injection energies, where the linear increase is observed and electron travel ballistically in any case. Thus, in fact, no additional fitting parameters are used. For this calculation, it is important that the detector size $\lambda_F \ll L\phi$. As one can see from Fig. 7, the divergence between the relaxation-time approximation and the experiment is only due to specific two-dimensional effects and reaches a maximum in the vicinity of $V_i = 3$ mV, where on the one hand a number of the scattered particles is comparable with the number of pure ballistic, and on the other hand scattering is still small-angular.

VII. CONCLUSIONS

We have studied the role of different groups of electrons on the propagation of electron beams in a high-mobility two-dimensional electron-gas for wide range of excess energies. We have observed a non-monotonic dependence of the detector signal on the excess energy of the injected electrons. This result can be explained in the framework of our model, separating the beam electrons into two groups, i.e. "quasiballistic" electrons and "heating" electrons (high-energy part of a beam). We have shown that due to the reduced dimensionality of the system the quasiballistic fraction consists not only of purely ballistic electrons but also of a significant number of electrons which have experienced small-angle electron-electron scattering events.

The small-angle character of electron-electron scattering is essentially a two-dimensional effect, predicted earlier by us [8,9,11], which manifests itself in the experiments discussed here. In addition, we have formulated the conditions where 2D effects can be best observed and thus electron-beam propagation over very long distances should be possible.

ACKNOWLEDGMENTS

This work was supported by the Volkswagen-Stiftung (Grant No. I/72 531), and by the DFG MO 771/1-2.

-
- [1] A. Yacoby, U. Sivan, C. P. Umbach, J. M. Hong, Phys. Rev. Lett. **66**, 1938 (1991).
- [2] A. Palevsky, M. Heiblum, C. P. Umbach, C. M. Knoedler, A. N. Broers, R. H. Koch, Phys. Rev. Lett. **65**, 1776 (1989).
- [3] L. W. Molenkamp, M. J. Brugmans, H. van Houten and C. T. Foxon, Semicond. Sci. Technol. **7**, B228 (1992).
- [4] F. Müller, B. Lengeler, Th. Schäpers, J. Appenzeller, A. Förster, Th. Klocke, and H. Lüth, Phys. Rev. B **51**, 5099 (1995); Th. Schäpers, M. Krüger, J. Appenzeller, A. Förster, B. Lengeler, and H. Lüth, Appl. Phys. Lett. **66**, 3603 (1995).
- [5] D. R. S. Cumming, J. H. Davies, Appl. Phys. Lett. **69**, 3363 (1996).
- [6] G. F. Giuliani, and J. J. Quinn, Phys. Rev. B **26**, 4421 (1982).
- [7] R. N. Gurzhi, A. N. Kalinenko, A. I. Kopeliovich, Phys. Rev. Lett. **74**, 3872 (1995).
- [8] R. N. Gurzhi, A. N. Kalinenko, A. I. Kopeliovich, Phys. Rev. B **52**, 4744 (1996).
- [9] R. N. Gurzhi, A. N. Kalinenko, A. I. Kopeliovich, Fiz. Nizk. Temp. **23**, 58 (1997) [Low Temp. Phys. **23** 44, (1997)].
- [10] R. N. Gurzhi, A. N. Kalinenko, A. N. Kopeliovich, Surface Science **361/362**, 497 (1996).
- [11] H. Buhmann, R. N. Gurzhi, A. N. Kalinenko, A. I. Kopeliovich, L. W. Molenkamp, A. V. Yanovsky, Fiz. Nizk. Temp. **24**, 978 (1998) [Low Temp. Phys. **24** 737, (1998)].
- [12] M. J. M. de Jong, and L. W. Molenkamp, Phys. Rev. B **51**, 13389 (1995).
- [13] A. V. Chaplik, Zh. Eksp. Teor. Fiz. **60**, 1845 (1971) [Sov. Phys.-JETP **33**, 997 (1971)].
- [14] L. W. Molenkamp, H. van Houten, C. W. J. Beenakker, R. Eppenga and C. T. Foxon, Phys. Rev. Lett. **65**, 1052 (1990).
- [15] L. W. Molenkamp, A. A. M. Staring, C. W. J. Beenakker, R. Eppenga, C. E. Timmering, J. G. Williamson, C. J. P. M. Harmans, C. T. Foxon, Phys. Rev. B **41**, 1274 (1990).
- [16] Note that while the thermopower of a quantum point-contact in linear response reaches a maximum in-between conductance plateaus, and is close to zero near the middle of a plateau [14], one expects through thermal broadening effects also a sizeable thermovoltage contribution for the adjustment of our detector point-contact at a large enough temperature difference
- [17] H. van Houten, L. W. Molenkamp, C. W. J. Beenakker, and C. T. Foxon, Semicond. Sci. Technol. **7**, B215 (1992).